

Colloidal Au Single-Atom Catalysts Embedded on Pd Nanocluster

Haijun Zhang^{*1}, Keisuke Kawashima², Mitsutaka Okumura³, and Naoki Toshima^{2*}

¹. *The State Key Laboratory of Refractory and Metallurgy, Wuhan University of Science and Technology, Wuhan, Hubei Province 430081, China*

². *Department of Applied Chemistry, Tokyo University of Science Yamaguchi, SanyoOnoda, Yamaguchi 756-0884, Japan*

³. *Graduate School of Science, Osaka University, Machikaneyama, Toyonaka, Osaka 560-0043, Japan*

*Corresponding authors, E-mail: toshima@rs.tus.ac.jp; zhanghaijun@wust.edu.cn

Table S1 Preparation conditions of Au₅₅Pd₅₅ catalyst using various kinds of Pd NCs as mother clusters

| BNCs | Pd mother clusters | Preparation conditions of Au | |
|-------|----------------------------------|---|---------------------|
| | | Molar ratio of starting materials | Reaction conditions |
| SA-S1 | Pd(1h) 90°C, $R_{PVP}=100$ | Au ³⁺ /Pd =55/55, PVP/Au ³⁺ =100, C ₆ H ₈ O ₆ /Au ³⁺ =20/1 | 95°C/0.25 h |
| SA-S2 | Pd(0.5h) 90°C, $R_{PVP}=100$ | | |
| SA-S3 | Pd(0.25h) 90°C, $R_{PVP}=100$ | | |

Table S2 Comparison between theoretical and ICP results of Pd and Au content for the Au₅₅Pd₅₅ catalyst prepared with various kinds of Pd NCs as mother clusters.

| BNCs | Pd mother clusters | Au content in final Au ₅₅ Pd ₅₅ | |
|-------|----------------------------------|---|--------|
| | | BNCs, atomic% | |
| | | Theoretical | ICP Au |
| SA-S1 | Pd(1h) 90°C, $R_{PVP}=100$ | 50 | 49.1 |
| SA-S2 | Pd(0.5h) 90°C, $R_{PVP}=100$ | 50 | 47.7 |
| SA-S3 | Pd(0.25h) 90°C, $R_{PVP}=100$ | 50 | 48.6 |

Table S3 Preparation conditions of series of colloidal Au/Pd SACs with various compositions under conditions of 95°C/0.25 h by successive reduction.

| BNCs | Pd mother clusters | Preparation conditions of Au | |
|------|----------------------------------|-----------------------------------|---|
| | | Molar ratio of starting materials | Reaction conditions |
| SA-1 | Pd(0.25h) 90°C, $R_{PVP}=100$ | $Au^{3+}/Pd = 3/55$ | 95°C/0.25 h PVP/ $Au^{3+} = 100/1$ (molar ratio), $C_6H_8O_6/Au^{3+} = 20/1$ (molar ratio); |
| SA-2 | | $Au^{3+}/Pd = 6/55$ | |
| SA-3 | | $Au^{3+}/Pd = 14/55$ | |
| SA-4 | | $Au^{3+}/Pd = 28/55$ | |
| SA-5 | | $Au^{3+}/Pd = 55/55$ | |
| SA-6 | | $Au^{3+}/Pd = 92/55$ | |

Table S4 Comparison between theoretical and ICP results of Pd and Au content for the final Au/Pd SACs prepared with various compositions.

| BNCs | Au/Pd | Au content in final Au-on-Pd catalysts, atomic% | |
|------|-------|---|-----|
| | | Theoretical | ICP |
| SA-1 | 3/55 | 5.2 | 4.2 |

| | | | |
|------|-------|------|------|
| SA-2 | 6/55 | 9.8 | 7.8 |
| SA-3 | 14/55 | 20.3 | 21.9 |
| SA-4 | 28/55 | 33.7 | 32.1 |
| SA-5 | 55/55 | 50.0 | 48.6 |
| SA-6 | 92/55 | 62.6 | 60.3 |

Table S5 Calculated adsorption energy of Au/Pd SACs by DFT

| Clusters | Calculated energy, Hartree | Spin | Crystalline facet | Adsorption energy DE, kJ/mol |
|----------------------------------|----------------------------|---------|-------------------|------------------------------|
| Au | -18398.30535 | doublet | - | - |
| Pd ₅₅ | -281493.5502 | singlet | - | - |
| Pd ₅₅ Au ₆ | -391883.6299 | singlet | {100} | 108.5 |
| Pd ₅₅ Au ₈ | -428680.5149 | singlet | {111} | 171.5 |

(In the case of Pd₅₅Au₆ system, for example, the adsorption energy DE was calculated by the

following equation: $DE = [E(\text{Pd}_{55}) + E(\text{Au}) \times 6 - E(\text{Pd}_{55}\text{Au}_6)] / 6$.)

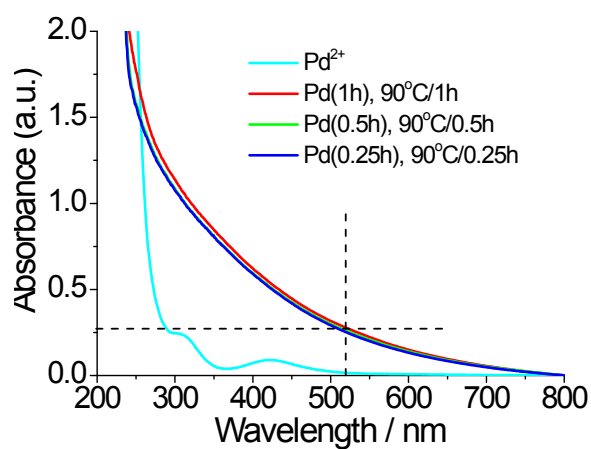
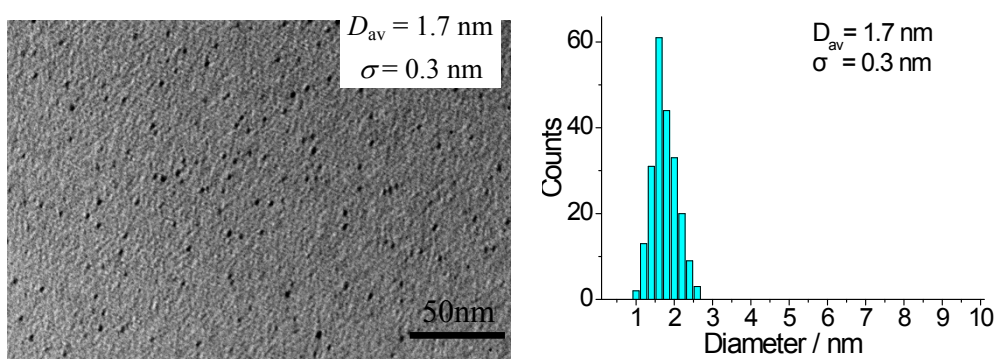
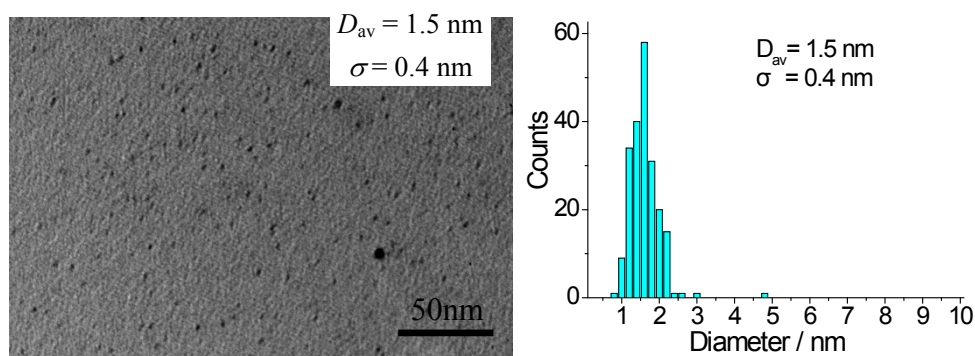


Figure S1. UV-Vis spectra of colloidal dispersions of Pd(1h), Pd(0.5h) and Pd(0.25h) mother NCs.

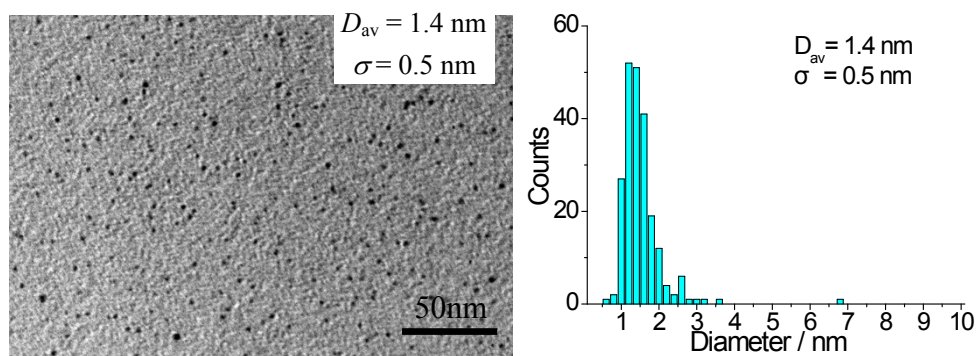
In order to get the best conditions for preparing the mother Pd NCs with tiny size, the reaction time was varied as a parameter. A series of the Pd NCs prepared were used as mother clusters for the preparation of the Au/Pd SACs. Figure S1 shows UV-Vis spectra of aqueous dispersions of Pd²⁺ ions and the Pd mother clusters prepared at 90°C for various periods. All the spectra of Pd NCs exhibit completely different shapes from that of Pd²⁺ ions and featureless and monotonously increasing absorbance toward higher energies, indicating that Pd²⁺ ions are completely reduced to Pd NCs under the present preparation conditions.



(a) Pd(1h), 90°C/1h



(b) Pd(0.5h), 90°C/0.5h



(c) Pd(0.25h), 90°C/0.25h

Figure S2. The TEM micrographs and size distribution histograms of the three kinds of Pd mother NCs prepared under 90°C for various hours.

The TEM image and size distribution histogram of the PVP-protected Pd mother NCs are shown in Figure S2. The distribution of the particle diameters of these three kinds of Pd mother clusters is nearly symmetric. The average sizes (\pm standard deviation) based on the TEM images (Figure S2) are 1.7 ± 0.3 nm for Pd(1h) NCs, 1.5 ± 0.4 nm for Pd(0.5h) NCs, and 1.4 ± 0.5 nm for Pd(0.25h) NCs, respectively. The results show that the average size of Pd mother clusters decrease with decreasing the reflux time. In the case of the Pd(0.25h) NCs mother clusters, the population of the PVP-protected Pd NCs has a peak at a diameter of about 1.4 nm, indicating that the Pd mother NCs consist of about 55 atoms in a particle on the average. We characterize this as the size-selected Pd_N (where N=55) NCs, where Pd₅₅ is known to be a possible ‘magic number’ cluster [S1]. The Pd₅₅ NC with the ideal size of about 1.4 nm can be characterized as a truncated octahedron with eight triangular {111} faces and six square {100} faces (Figure 1). The mean particle diameters were used for the approximate calculation and preparation of the PVP-protected colloidal Au/Pd SACs in the following steps. Here, we simply consider that all the prepared ‘Pd mother clusters’ possess the ideal structure of Pd₅₅, and that the defect sites including kink atoms, twinning boundaries, and

stacking faults are not taken into consideration.

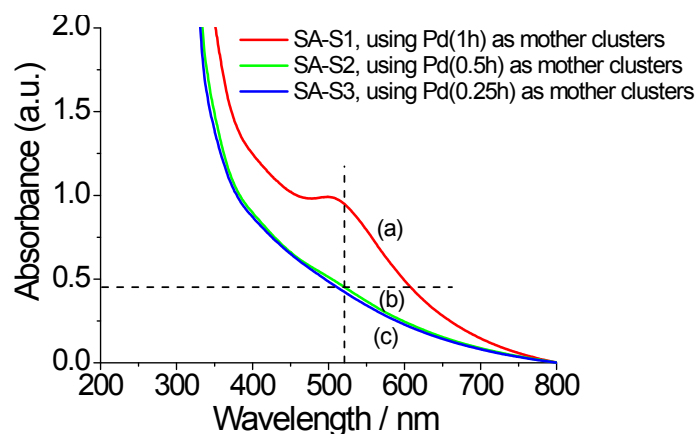
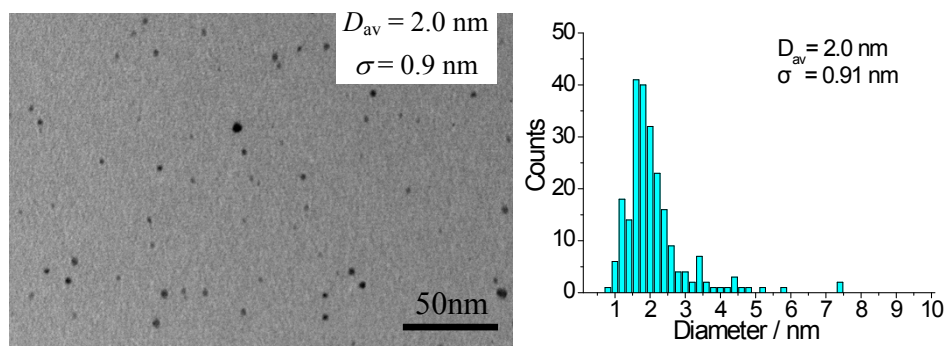


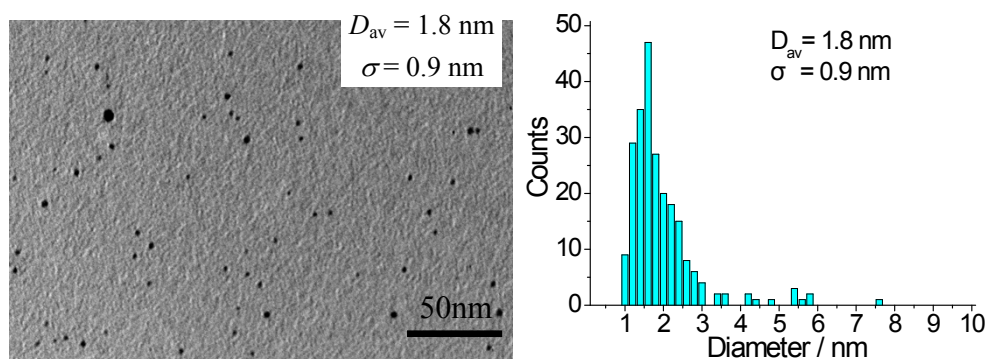
Figure S3. UV-Vis spectra of colloidal dispersions of three kinds of Au₅₅Pd₅₅ catalyst prepared by successive reduction using *L*-ascrobic acid as reducing reagent (Three kinds of Pd NCs of Pd(1h), Pd(0.5h) and Pd(0.25h) were used as mother clusters. All the Au₅₅Pd₅₅ catalysts were prepared under conditions of 95°C/0.25 hour.).

Three kinds of Au₅₅Pd₅₅ (the atomic ratio of Au : Pd = 55 : 55) catalysts using Pd(0.25h), Pd(0.5h), and Pd(1h) NCs, respectively, as mother clusters were synthesized at first. The UV-Vis absorption spectra of the aqueous dispersions of three kinds of Au₅₅Pd₅₅ catalysts are shown in Figure S3. The spectrum of the Au₅₅Pd₅₅ dispersion prepared from Pd(1h) NCs as mother clusters exhibits a small peak at 520 nm, attributed to the surface plasmon resonance of the metallic Au. In the case of other two series of catalysts, their spectra exhibit a featureless and monotonously increasing absorbance toward higher energies. Comparing Figure S3 with Figure S1 can give the following findings: 1) The absorbance intensities of prepared Au₅₅Pd₅₅ catalysts are higher than that of Pd mother NCs although the metal nanoparticle concentrations in the two dispersions are almost same, which means that the surface compositions are changed from the original Pd mother NCs, i.e. Au is deposited on the surface of Pd mother NCs. 2) It is suggested that large Pd mother NCs

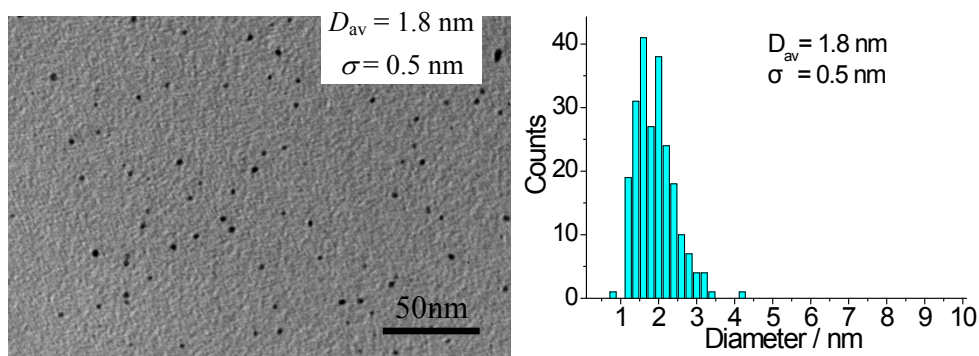
(Pd(1h)) can catch a larger amount of Au atoms, which form larger Au clusters on the surface of Pd NC (as shown in curve (a) of Figure S3). This can be explained as follows: The TEM results (Figure S4) show that the size of Pd(1h) NCs is larger than those of Pd(0.5h) and Pd(0.25h) NCs, and that, on the other hand, the ratios of Au/Pd are the same for the prepared Au₅₅Pd₅₅ catalysts. Thus, it is reasonably suggested that the number of Au atoms deposited on the surface of large Pd NCs (for example, Pd(1h) NCs) should be more than those of relatively small Pd NCs (Pd(0.5h) and Pd(0.25h)). It is well known that large amount of Au formed on the surface of Pd mother NCs would easily result in the aggregation of Au atoms and that the bigger aggregates could provide the stronger absorbance. Thus, the absorbance intensity of curves in Figure S3 decreases in the following order: Au₅₅Pd(1h)₅₅ > Au₅₅Pd(0.5h)₅₅ > Au₅₅Pd(0.25h)₅₅.



(a) SA-S1, using Pd(1h) as mother clusters



(b) SA-S2, using Pd(0.5h) as mother clusters



(c) SA-S3, using Pd(0.25h) as mother clusters

Figure S4. The TEM micrographs and size distribution histograms of Au₅₅Pd₅₅ catalysts prepared using Pd(1h), Pd(0.5h) and Pd(0.25h) as mother clusters (The Au₅₅Pd₅₅ catalysts were synthesized using *L*-ascrobic acid as reducing reagent under conditions of 95°C/0.25 hour.).

Figure S4 shows representative TEM images and size distribution histograms of Au₅₅Pd₅₅ catalysts prepared with various Pd NCs as mother clusters. The average sizes (\pm standard deviation) of Au₅₅Pd₅₅ catalysts prepared by using Pd(0.25h), Pd(0.5h), and Pd(1h) NCs as mother clusters were estimated to be 1.8 ± 0.5 nm, 1.8 ± 0.9 nm, and 2.0 ± 0.9 nm, respectively, based on the TEM images, indicating that the mean particle diameter initially decreased from 2.0 nm to the smallest (1.8 nm) with decreasing the reflux time of Pd mother clusters from 1.0 to 0.25 h. Comparing Figure S4 with Figure S2, it can be found that the produced Au₅₅Pd₅₅ catalysts had larger average particle sizes than the corresponding Pd mother clusters, suggesting that Au atoms are indeed deposited on the surface of Pd NCs. These results are also supported by the ICP analysis of the prepared Au₅₅Pd₅₅ catalysts. The chemical compositions of the Au₅₅Pd₅₅ catalysts were obtained from the ICP analysis as shown in Table S2. Comparison of the Au atomic% in the final catalysts and that in the metal precursor feed indicates that the atomic ratio of Au in the feed in the synthetic solution was approximately equal to that in the final catalysts.

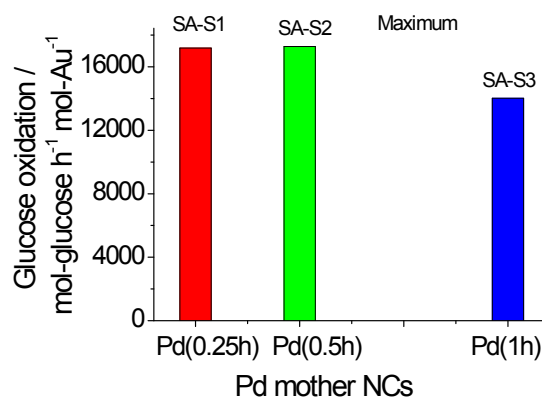


Figure S5. Catalytic activity for glucose oxidation of Au₅₅Pd₅₅ catalysts prepared using various kinds of Pd NCs as mother clusters. (Three kinds of Pd NCs of Pd(1h), Pd(0.5h) and Pd(0.25h) were used as mother clusters. The Au₅₅Pd₅₅ catalysts were prepared by successive reduction using *L*-ascrobic acid as reducing reagent under conditions of 95°C/0.25 hour.)

The prepared Au₅₅Pd₅₅ catalysts were used as the catalyst for the aerobic oxidation of glucose in water at 60°C. Their catalytic activity increased in the order Au₅₅Pd(1h)₅₅ < Au₅₅Pd(0.5h)₅₅ ≈ Au₅₅Pd(0.25h)₅₅ (Figure S5). The highest catalytic activity of about 17,200 mol-glucose·h⁻¹·mol-Au⁻¹ was achieved for the smallest Au₅₅Pd₅₅ catalysts prepared using Pd(0.5h) and Pd(0.25h) NCs as mother clusters. The above experimental results show that Au₅₅Pd₅₅ catalysts with small average diameter and high catalytic activity for aerobic glucose oxidation can be obtained by using Pd(0.25h) NCs as mother clusters. The results confirm again that Au atoms would be more easily distributed on the surface of the mother clusters with small size than that with large size, which is also supported by the UV-Vis results shown in Figure S3.

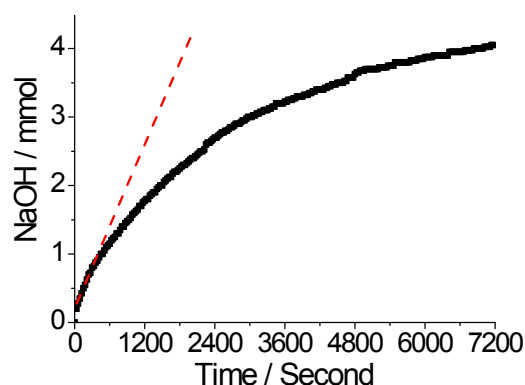
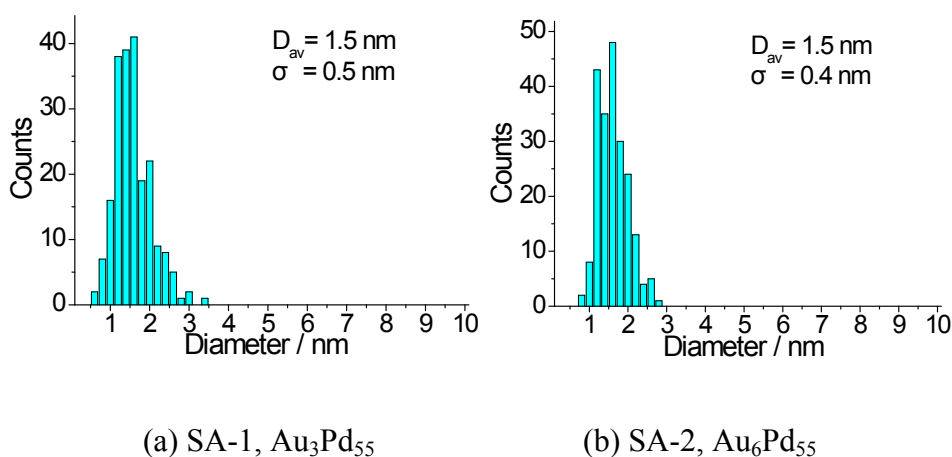
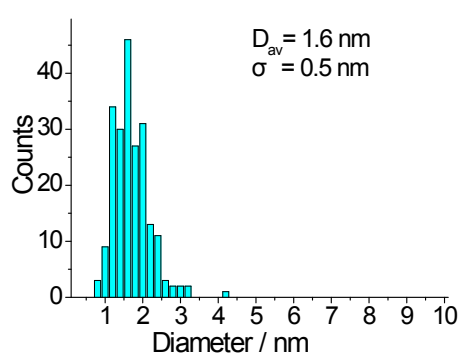


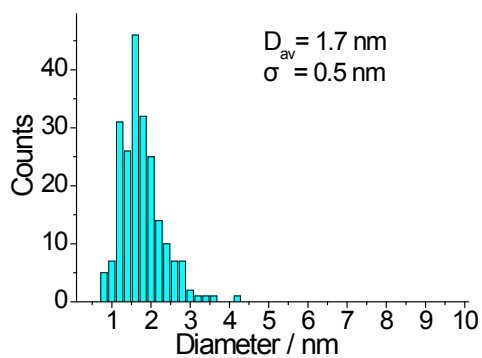
Figure S6. The typical NaOH amount vs reaction time curve for glucose oxidation catalyzed by $\text{Au}_3\text{Pd}_{55}$ SAC. The erupting period is observed, the red das line is shown to fit the curve for determination of the simultaneous maximum activity. [glucose] / [M] \cong 44, 400, mol ratio; pH=9.5; 60 °C.

The activity ($\text{mol-glucose}\cdot\text{h}^{-1}\cdot\text{mol-M}^{-1}$) was calculated from the slope of a straight line fitted using the NaOH amount vs reaction time curve. The initial specific activity related to the metal content of the catalysts was calculated for comparison. A typical NaOH amount vs time diagram with the fit line is shown in Figure S6. The slope of the fit line reflects the initial activity of the catalyst.

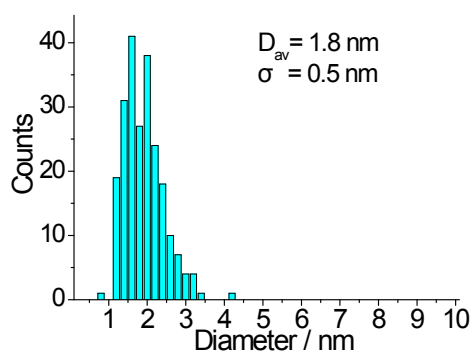




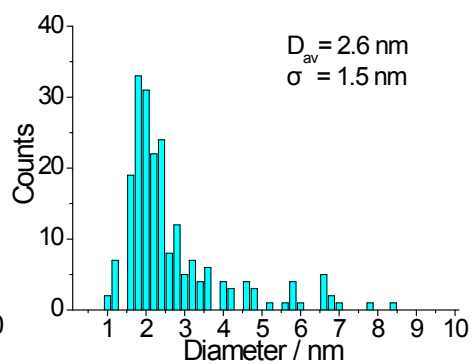
(c) SA-3, Au₁₄Pd₅₅



(d) SA-4, Au₂₈Pd₅₅

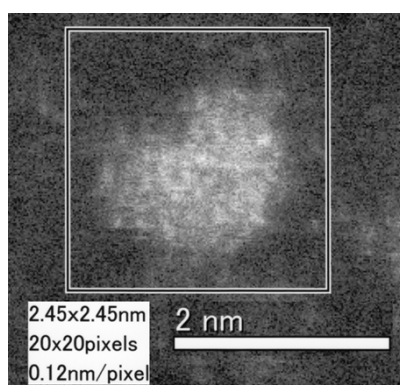


(e) SA-5, Au₅₅Pd₅₅

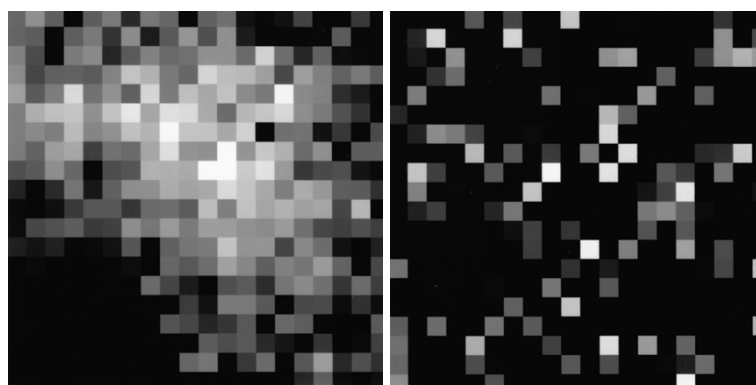


(f) SA-6, Au₉₂Pd₅₅

Figure S7. The size distribution histograms of colloidal Au/Pd SACs prepared with various compositions.



(a) HAADF-STEM of a NC of SA-1



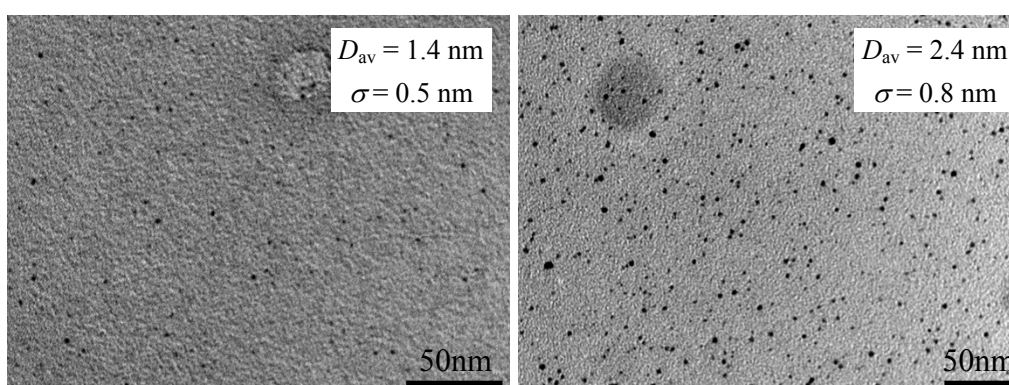
EELS of Pd

EELS of Au

(b) Surface atomic configurations of a cluster of SA-1

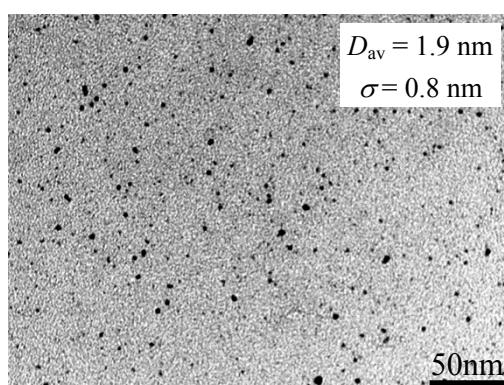
Figure S8. HAADF-STEM image and EELS mapping of a $\text{Au}_3\text{Pd}_{55}$ SAC NC. (a) HAADF-STEM

image of a single $\text{Au}_3\text{Pd}_{55}$ SAC NC (b) EELS mapping of a $\text{Au}_3\text{Pd}_{55}$ SAC NC.



(a) Au NCs

(b) Au/Pd (2/8) NCs



(c) Au/Pd (7/3) NCs

Figure S9. TEM micrographs and size distributions of Au NCs (a) Au/Pd (2/8) NCs (b) and Au/Pd

(7/3) NCs (c) prepared by rapid injection of NaBH_4 .

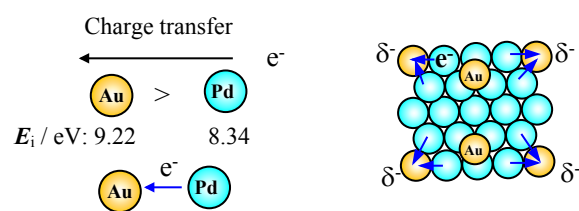


Figure S10. Schematic illustration of electronic charge transfer effects in Au_8Pd_5 SACs (E_i : Ionization energy.).

[S1] Jongh, L. J.; Baak, J.; Brom, H. B.; Putten, D. V. D. in: P. Jena, S. N. Khanna, B. K. Rao (Eds.), Physics and chemistry of fine systems: From clusters to crystals, Kluwer, Dordrecht, 1992, vol. II, p. 839.